

The Difference Between the Narrow Line Region of Seyfert 1 and Seyfert 2 Galaxies

Henrique R. Schmitt^{1,2,3}

ABSTRACT

This paper presents a comparative study of emission line ratios of the Narrow Line Region (NLR) of Seyfert 1 and Seyfert 2 galaxies. It includes a literature compilation of the emission line fluxes $[\text{OII}]\lambda 3727\text{\AA}$, $[\text{NeIII}]\lambda 3869\text{\AA}$, $[\text{OIII}]\lambda 5007\text{\AA}$ and $[\text{NeV}]\lambda 3426\text{\AA}$, as well as $60\mu\text{m}$ continuum flux, for a sample of 52 Seyfert 1's and 68 Seyfert 2's. The distribution of the emission line ratios $[\text{OII}]/[\text{NeIII}]$ and $[\text{OII}]/[\text{NeV}]$ shows that Seyfert 1's and Seyfert 2's are statistically different, in the sense that Seyfert 1's have values smaller than those of Seyfert 2's, indicating a higher excitation spectrum. These and other emission line ratios are compared with sequences of models which combine different proportions of matter and ionization bounded clouds and also sequences of models which vary only the ionization parameter. This comparison shows that the former models reproduce better the overall distribution of emission line ratios, indicating that Seyfert 1's have a smaller number of ionization bounded clouds than Seyfert 2's. This difference, together with other results available in the literature, are interpreted from the point of view of four different scenarios. The most likely scenario assumes that Seyfert 1's have NLR's smaller than those of Seyfert 2's, possibly due to a preferential alignment of the torus axis close to the host galaxy plane axis in Seyfert 1's.

Subject headings: galaxies:Seyfert — galaxies:active — galaxies:nuclei

1. Introduction

The observation of broad polarized lines in the spectrum of the Seyfert 2 galaxy NGC1068 (Antonucci & Miller 1985) showed that Seyfert 2's can be Seyfert 1's where the direct view of the central engine is blocked. This is the basis for the Unified Model of AGN's, which assumes that objects of different activity class, like Seyfert 1's and Seyfert 2's, are the same kind of object, surrounded by a dusty molecular torus. The orientation of this torus relative to the line of sight determines whether the AGN is observed as a broad lined object (Seyfert 1), where the nuclear engine is seen through the torus opening, or as a narrow lined object (Seyfert 2), where our view of the central engine and consequently the broad lines, is blocked by the torus.

Several pieces of observational evidence supporting this scenario have been obtained during the last decade, the strongest one being the observation of polarized broad emission lines in the spectrum of several Seyfert 2 galaxies (Antonucci & Miller 1985; Miller & Goodrich 1990; Kay 1994; Tran 1995). The observation of collimated radiation escaping the nuclear region of Seyfert 2's, seen as cone like emission line

¹Depto. Astronomia, IF-UFRGS, CP 15051, CEP 91501-970, Porto Alegre, RS, Brazil

²CNPq Fellow

³email:schmitt@if.ufrgs.br

regions (Pogge 1988a,b, 1989; Schmitt, Storchi-Bergmann & Baldwin 1994, Schmitt & Storchi-Bergmann 1996, and references therein), or linear radio structures (Ulvestad & Wilson 1984a,b, 1989), also suggest that the direct view of the central engine is blocked in these objects. More direct evidence for the obscuration of the central engine in Seyfert 2's comes from the analysis of X-ray spectra, which show large absorbing column densities in these objects (Mulchaey, Mushotzky & Weaver 1992). Also, the observation of H₂O masers very close to the nucleus of some Seyfert 2's, like NGC1068 and NGC4258 (Miyoshi 1995, Gallimore 1996, Greenhill 1996), show the presence of large concentrations of molecular gas, hiding the central engine.

Recent papers, however, present some results suggesting that not only the orientation of the circumnuclear torus relative to the line of sight, but also its orientation relative to the host galaxy may be important in the AGN classification. It was known since Keel (1980), that there is a paucity of Seyfert 1's with edge-on host galaxies. This result was later confirmed by Maiolino & Rieke (1995) and Simcoe et al. (1997), who suggested that, in some cases, dust along a Seyfert 1 galaxy disk may be responsible for the obscuration of the broad lines (making it appear as a Seyfert 2). Moreover, Schmitt et al. (1997) presented a comparison between the linear radio structure of Seyfert galaxies, with their host galaxy major axis. They found that the radio structures are more likely to be aligned close to the host galaxy plane axis in Seyfert 1's, but can have any direction in Seyfert 2's, confirming the result by Maiolino & Rieke (1995). Another result that corroborates this scenario is the observation that the NLR of Seyfert 1's usually is much smaller than that of Seyfert 2's, when they are compared as if Seyfert 2's were observed pole-on, in the same way as Seyfert 1's (Schmitt & Kinney 1996). The smaller Seyfert 1 NLR's can be understood if these objects have their torus axis preferentially aligned close to the host galaxy plane axis, where there is less gas to be ionized.

The above results show differences between the NLR of Seyfert 1 and Seyfert 2 galaxies and point towards older papers, where some other differences have also been detected. Heckman & Balick (1979) and Shuder & Osterbrock (1981) showed that the ratio [OIII]4363/5007 is larger in Seyfert 1's than in Seyfert 2's. This result indicates that the [OIII] zone of Seyfert 1's, when compared to Seyfert 2's, have larger temperatures and/or densities. Yee(1980) and Shuder (1981) showed that the emission lines, [OIII], [OII] and [OI], are more luminous in Seyfert 2's relative to Seyfert 1's of similar optical luminosity, consistent with the torus blocking part of the continuum light in Seyfert 2's. Shuder & Osterbrock (1981) and Cohen (1983) showed that the emission line ratios [FeVII]/H β and [FeX]/H β are larger in Seyfert 1's than in Seyfert 2's, indicating that Seyfert 1's have higher excitation. Yet another interesting result was obtained by De Robertis & Osterbrock (1986 and references therein), who showed that the FWHM of forbidden lines are well correlated with the ionization potential in Seyfert 1's, but not with the critical density for de-excitation, while in Seyfert 2's the opposite happens. They have also showed that these lines have smaller FWHM in Seyfert 1's than in Seyfert 2's, and that the [OI] line profiles show evidence of two components in Seyfert 2's, probably formed in two different regions.

This paper presents a compilation of literature data of the emission line fluxes [OII] λ 3727Å, [NeIII] λ 3869Å, [NeV] λ 3426Å and [OIII] λ 5007Å ([OII], [NeIII], [NeV] and [OIII], hereafter), as well as 60 μ m continuum fluxes for a sample of 52 Seyfert 1 and 68 Seyfert 2 galaxies. These lines are used to compare the excitation of the NLR gas in Seyfert 1's and Seyfert 2's, through the analysis of different emission line ratios. A simple interpretation of the Unified Scheme would suggest that the spectrum of the NLR of Seyfert 1's and Seyfert 2's should have similar degrees of excitation. However, as shown by the above papers, this may not be true. Effects like the possible obscuration of parts of the NLR by the torus, or the smaller NLR size in Seyfert 1's, could influence the average NLR excitation in these two classes of objects.

The paper is organized in the following way, Section 2 presents the sample, the reasons for the choice

of these emission lines and a discussion of the possible selection effects. Section 3 shows the results of the comparison between Seyfert 1’s and Seyfert 2’s. Section 4 shows the comparison between the data and photoionization models and discusses possible interpretations of the results, while Section 5 gives the summary.

2. The Data and Selection Effects

The usual way to analyze the gas excitation in galaxies is through the use of ratios between different emission line fluxes. The most common approach is to use BPT diagrams, which allow the differentiation between Seyfert 2’s, LINER’s and HII regions (Baldwin, Phillips & Terlevich 1981). These diagrams use emission line ratios like $[\text{OII}]/[\text{OIII}]$, $[\text{NII}]/\text{H}\alpha$ and $[\text{OIII}]/\text{H}\beta$, which can be easily measured in Seyfert 2 galaxies. However, due to blending with broad lines, as is the case for $\text{H}\beta$ and $\text{H}\alpha+[\text{NII}]$, these lines cannot be easily measured in Seyfert 1’s. Another problem is the difficulty in determining the internal reddening in Seyfert 1’s, which can considerably influence the $[\text{OII}]/[\text{OIII}]$ ratio.

In order to avoid the above problems, a different set of emission lines, easily measurable in both Seyfert 1 and Seyfert 2 galaxies, is chosen. These lines are: $[\text{OII}]\lambda 3727\text{\AA}$, $[\text{NeIII}]\lambda 3869\text{\AA}$, $[\text{NeV}]\lambda 3426\text{\AA}$ and $[\text{OIII}]\lambda 5007\text{\AA}$. They span a wide range in ionization potentials, are not blended with other lines, either broad or narrow and, with the exception of $[\text{OIII}]$, are close in wavelength, which minimizes scatter resulting from reddening effects and relative flux calibration errors. $[\text{NeIII}]$ is of particular interest, because its values of ionization potential and critical density for collisional de-excitation are very similar to those of $[\text{OIII}]$, implying that they may be formed in similar regions. In this way the ratio $[\text{OII}]/[\text{NeIII}]$ can be used in the place of $[\text{OII}]/[\text{OIII}]$ with the advantage of being reddening free. For more on the use of $[\text{NeIII}]$ in diagnostic diagrams, see Rola, Terlevich & Terlevich (1997).

The literature was searched for Seyfert 1 and Seyfert 2 galaxies with measured emission line fluxes of the lines $[\text{OII}]$, $[\text{NeIII}]$, $[\text{NeV}]$ and $[\text{OIII}]$. It was possible to find 52 Seyfert 1 and 68 Seyfert 2 galaxies, which are shown in Tables 1 and 2, respectively. These Tables give the names of the objects, B magnitude, radial velocity, Morphological Type (de Vaucouleurs et al. 1991, Mulchaey 1994), the emission line ratios $[\text{OII}]/[\text{NeIII}]$, $[\text{OII}]/[\text{NeV}]$, $[\text{NeIII}]/[\text{NeV}]$ and $[\text{OII}]/[\text{OIII}]$, the IRAS $60\mu\text{m}$ flux, the reference from which the emission line ratios were obtained and the aperture size used to observe the spectrum. Notice that it was not possible to find $[\text{NeV}]$ and $60\mu\text{m}$ flux, as well as Morphological Type for all galaxies in the sample.

An important point about the data collection is that, for every object, emission line fluxes from two different references were never mixed. Also, preference was given to data obtained with medium size aperture ($3''\text{--}7''$), in order to include as much NLR emission as possible, but also avoid extremely large aperture sizes, which could include HII regions in the galaxy disk. The apertures given in Tables 1 and 2 were classified in 3 categories, S (small), corresponding to apertures smaller than $3''$, M (medium), corresponding to apertures in the range $3''\text{--}7''$ and L (large), corresponding to apertures larger than $7''$.

The radial velocities and aperture sizes (in arcseconds) were used to calculate the metric aperture sizes, which correspond to the dimension of the aperture in the galaxy (in parsecs), calculated assuming $H_0 = 75 \text{ km s}^{-1} \text{ Mpc}^{-1}$. These values were calculated by taking the square root of the slit area and, when comparing the average metric aperture sizes for Seyfert 1’s and Seyfert 2’s, it was found that they have similar values, with means and 1σ uncertainties of $1972\pm 1578 \text{ pc}$ and $2008\pm 2101 \text{ pc}$, respectively. The Spearman rank test was used to compare the four emission line ratios with the metric aperture sizes. They do not show any correlation, confirming that aperture effects are not a problem for the analysis.

Since the sample was obtained from the literature, rather than selected from an isotropic property, it is necessary to check if both Seyfert 1 and Seyfert 2 galaxies have similar intrinsic properties. First it was checked if Seyfert 1's and Seyfert 2's have similar luminosities and are not biased towards high luminosity Seyfert 1's and low luminosity Seyfert 2's, which could imply a larger flux of high excitation lines in Seyfert 1's. This test was done by comparing the $60\mu\text{m}$ luminosities of the two groups of galaxies. Here it was assumed that the $60\mu\text{m}$ luminosity is nuclear radiation absorbed by the circumnuclear torus and reradiated in the far-infrared, so it should scale with total luminosity. However, notice that it can depend on the torus covering factor, which can differ for Seyfert 1's and Seyfert 2's. Also, it should be noticed that the assumption that $60\mu\text{m}$ luminosity scale with the nuclear luminosity must be taken with care, because, as pointed out by Pier & Krolik (1992), the torus emission may be anisotropic even at $60\mu\text{m}$.

The results for this comparison are shown in Figure 1, where it can be seen that both groups have similar distributions, with the Kolmogorov-Smirnov (KS) test showing that two samples drawn from the same parent population would differ this much 44% of the time. Table 3 gives the number of Seyfert 1 and Seyfert 2 galaxies with $60\mu\text{m}$ luminosity available, their mean values, standard deviations, and the KS test probability. This Table also gives information about other results from the KS tests done below. The four emission line ratios were also compared with the $60\mu\text{m}$ luminosity, but the Spearman rank test did not show any correlation. It should be noticed, however, that not all galaxies have IRAS $60\mu\text{m}$ flux available, only 40 out of 52 Seyfert 1's and 52 out of 68 Seyfert 2's.

The second test checks whether the two groups have similar morphological types and are not biased towards Seyfert 2's in late type galaxies. Late type galaxies are more likely to have circumnuclear HII regions, which usually have much stronger [OII] than [NeIII] fluxes, and would make Seyfert 2's look like lower excitation objects. Figure 2 shows the distribution of morphological types, where it can be seen that both groups have similar distributions, with the KS test showing that two samples drawn from the same parent population would differ this much 99.86% of the time, in other words, would be more alike only 0.14% of the time.

3. Results

Figure 3 shows the histogram of [OII]/[NeIII], where it can be seen that Seyfert 1's have, on average, smaller values than those of Seyfert 2's, indicating a higher excitation spectrum. Of particular interest in this histogram is the double cut-off in the distribution, for [OII]/[NeIII]<1 there are 12 Seyfert 1's and only 2 Seyfert 2's, while for values [OII]/[NeIII]>3.5 there are only Seyfert 2's. Table 3 shows the result of the KS test for this emission line ratio, which shows that two samples drawn from the same parent population would differ this much 0.02% of the time.

Figure 4 shows the histogram of [OII]/[NeV]. As for [OII]/[NeIII], Seyfert 1's again are displaced towards values smaller than those found in Seyfert 2 galaxies. For [OII]/[NeV]<1 there are 17 Seyfert 1's and only 1 Seyfert 2. However, for this line ratio there is not a high cut-off value, above which only Seyfert 2's are found, as is the case for [OII]/[NeIII]. The KS test shows that two samples drawn from the same parent population would differ this much only 0.16% of the time. It should be noticed that it was only possible to find [NeV] fluxes for approximately 45% of the galaxies in the sample. This is due in part to the fact that not all detectors have a good sensitivity below $\lambda 3700\text{\AA}$ and to the fact that most of the NLR studies are centered on emission lines above $\lambda 3700\text{\AA}$. Also, care must be taken when analyzing emission line ratios involving [NeV], because the detection of this line can be biased towards high excitation objects.

Figure 5 shows the distribution of $[\text{NeIII}]/[\text{NeV}]$. Besides the fact that there are 7 Seyfert 1 and no Seyfert 2 galaxies with $[\text{NeIII}]/[\text{NeV}] < 0.5$, the two distributions are approximately similar, with the KS test showing that two samples drawn from the same parent population would differ this much only 11% of the time. However, as stated above, this result should be taken with care, because it includes the $[\text{NeV}]$ line.

The histogram of $[\text{OII}]/[\text{OIII}]$ is shown in Figure 6, where it can be seen that Seyfert 1's and Seyfert 2's have a similar distribution of values. The KS test shows that two samples drawn from the same parent population would differ this much only 23% of the time. This emission line ratio is shown here because it is one of the most common indicators of gas excitation. However, due to the large wavelength difference between the two lines ($\approx 1300\text{\AA}$), this ratio is extremely dependent on internal reddening and even the small value of internal reddening $E(B-V)=0.2$ makes the $[\text{OII}]/[\text{OIII}]$ ratio increase by $\approx 20\%$. As discussed above, $[\text{NeIII}]$ originates in regions similar to $[\text{OIII}]$ and the $[\text{OII}]/[\text{NeIII}]$ ratio can substitute $[\text{OII}]/[\text{OIII}]$.

4. Discussion

4.1. Photoionization Models

The results presented in the previous section show that the average excitation of the NLR of Seyfert 1's is larger than that of Seyfert 2's. This result is interpreted using diagnostic diagrams involving the emission line ratios studied in this paper. Figures 7a,b,c show the diagrams $\text{Log } [\text{OII}]/[\text{NeV}] \times \text{Log } [\text{OII}]/[\text{NeIII}]$, $\text{Log } [\text{NeIII}]/[\text{NeV}] \times \text{Log } [\text{OII}]/[\text{NeIII}]$ and $\text{Log } [\text{OII}]/[\text{OIII}] \times \text{Log } [\text{OII}]/[\text{NeIII}]$, respectively. It can be seen that Seyfert 1's are more concentrated towards the lower left side in these diagrams, which correspond to a higher excitation, confirming the results obtained from Figures 3, 4, 5 and 6. These distributions of emission line ratios are compared with photoionization models, to analyze the possible origins of this difference in excitation.

These results can be interpreted from the point of view of models that combine different proportions of matter and ionization bounded clouds. In these models the matter bounded clouds produce most of the high excitation lines ($[\text{NeIII}]$, $[\text{OIII}]$ and $[\text{NeV}]$) and little of low excitation lines ($[\text{OII}]$ and $[\text{NII}]$), while the ionization bounded clouds produce most of the low ionization lines and little of high excitation lines. The use of such models was proposed by Viegas & Prieto (1992) to explain the emission line region of 3C227. Later Binette, Wilson & Storchi-Bergmann (1996) (BWSB96, hereafter) used models of this kind to study the extended NLR of Seyfert galaxies, showing their efficacy in the reproduction of high excitation lines, like $[\text{NeV}]\lambda 3426\text{\AA}$ and $\text{HeII}\lambda 4686\text{\AA}$, as well as the $[\text{OIII}]$ temperature, which has always been a problem for the traditional photoionization models which use sequences of ionization parameter.

Sequences of models adding different proportions of matter and ionization bounded clouds were calculated using the photoionization code MAPPINGS (Binette et al. 1993a,b), following the description given in BWSB96. The models were calculated using a power law ionizing spectrum of the form $F_\nu \propto \nu^\alpha$, and two different values of α were tested, -1.3 and -1.5 . The matter bounded clouds are ionized by this spectrum and the calculation stops when 40% of the incident spectrum is absorbed. The output, reprocessed spectrum from the matter bounded clouds, is the one that ionizes the ionization bounded clouds. The models also assume that the ionization bounded clouds leak some of the input radiation, in order to avoid overproduction of low ionization lines, like $[\text{OII}]$ and $[\text{NII}]$. In the case of $\alpha = -1.3$, it is assumed that the ionization bounded clouds allow 3% of the ionizing radiation to escape, while for $\alpha = -1.5$ this value is 10%.

The models were calculated considering an isobaric prescription, where the pressure is constant within any matter bounded or any ionization bounded cloud. The ionization parameter adopted for the matter bounded spectrum was $U=0.04$. Nevertheless, for the ionization bounded clouds of the $A_{M/I}$ sequence (see below), instead of specifying the ionization parameter, their pressure was fixed at 20 times that of the matter bounded clouds, as done by BWSB96. The adopted density was $n=50 \text{ cm}^{-3}$ and the gas metal abundance was solar ($Z=1$). It is also assumed that the gas is mixed with a small quantity of dust $\mu = 0.015^4$ and the abundance of metals in the grains is depleted from the gas. Notice that this is a very small amount of dust and, according to Binette et al. (1996), higher amounts of dust produce only minimal changes in the output spectrum of ionization bounded clouds but can have larger effects on the matter bounded clouds. However, the matter bounded clouds are not expected to have a large quantity of dust, because it can be easily destroyed by the radiation field. The only independent parameter in these models is the ratio between the solid angle subtended by matter bounded clouds, relative to the solid angle subtended by the ionization bounded clouds ($A_{M/I}$). Larger values correspond to a larger contribution from matter bounded clouds relative to ionization bounded clouds and vice-versa. This parameter was varied in the range $0.01 \leq A_{M/I} \leq 634$, in steps of 0.2 dex. These models are represented as a solid line in Figures 7a,b,c, with the value of α indicated beside the line.

In order to test the effects of other physical and chemical conditions, two other sequences of $A_{M/I}$ models were calculated. In the first one $\alpha = -1.5$, with the same parameters as above, but for gas with twice the solar metallicity ($Z=2$). In the second set of models $\alpha = -1.5$ and $Z=1$, but the density is 500 cm^{-3} . These models have the same range of $A_{M/I}$ as above, are shown as a long dashed lines in Figure 7a,b,c and are identified as $Z=2$ and $n=500 \text{ cm}^{-3}$, respectively.

Just for comparison with the above models, MAPPINGS was also used to calculate traditional sequences of models, varying only the ionization parameter. The parameters of the models were, power law ionizing spectrum with $\alpha = -1.3$, constant density $n=50 \text{ cm}^{-3}$, metallicity $Z=1$ and dust content $\mu = 0.015$. As for the $A_{M/I}$ models, two other sequences, one with $n=500 \text{ cm}^{-3}$ and $Z=1$, and the other with $n=50 \text{ cm}^{-3}$ and $Z=2$, were also tried. It was assumed that 3% of the ionizing radiation escape from the clouds, in order to avoid the overproduction of low ionization lines. The ionization parameter was varied in the range $-4 \leq \text{Log } U \leq -0.8$, in steps of 0.2 dex. The three sequences of models are very similar, the only exception being the sequence of models with $Z=2$ in the diagram $\text{Log}([\text{OII}]/[\text{OIII}]) \times \text{Log}([\text{OII}]/[\text{NeIII}])$ (Figure 7c), which are very similar to the $A_{M/I}$ sequence with $Z=2$. Due to this fact, only the sequence with $n=50 \text{ cm}^{-3}$ and $Z=1$ is presented as a dotted line in Figures 7a,b,c.

It can be seen in Figures 7a and b, that the $A_{M/I}$ sequences of models cover very well the observed distribution of values. In the case of Figure 7c, the diagram $\text{Log}([\text{OII}]/[\text{OIII}]) \times \text{Log}([\text{OII}]/[\text{NeIII}])$, these models have some problem to reproduce the observed distribution of values. It would be necessary to change other parameters, like the amount of dust in the models, the pressure jump between the matter and the ionization bounded clouds, or the amount of radiation which leaks from the ionization bounded clouds, in order to better reproduce the observed distribution of values. The fact that Seyfert 1's have $[\text{OII}]/[\text{NeIII}]$ and $[\text{OII}]/[\text{NeV}]$ values smaller than Seyfert 2's, can be interpreted as due to a smaller contribution from ionization bounded clouds, relative to matter bounded clouds, to the spectra of those objects. This comparison also shows that the $A_{M/I}$ models with $\alpha = -1.3$ are not as good a representation for the observed values as the ones with $\alpha = -1.5$, because they produce too much large fluxes of the higher excitation lines, like $[\text{NeV}]$.

⁴ μ is the dust to gas ratio of the clouds, in units of the solar neighborhood dust-to-gas ratio

The comparison with the traditional U sequence of models, shows that they are a poor representation of the data points, even when varying parameters like the gas abundance or density. Only in Figure 7c, where the $A_{M/I}$ sequence of models has some problems to represent the observed distribution of points, these models could be a better representation for the data. However, they require unconventionally large ionization parameters ($U > 0.01$).

4.2. Possible interpretations

Four possible interpretations for the above result are studied here.

1-) *Part of the matter bounded clouds (which produce most of [NeIII], [OIII] and [NeV]), is hidden by the circumnuclear torus in Seyfert 2's.* A similar problem was found by Jackson & Browne (1990) in the comparison of Quasars with Radio Galaxies. They show that the [OIII] emission of Quasars is much stronger than that of Radio Galaxies, proposing that part of the [OIII] emission is obscured by the torus in the latter objects. Hes, Barthel & Fosbury (1993) showed that, when comparing the [OII] emission of Quasars and Radio Galaxies, which comes from a less obscured, lower excitation region, both classes of objects have very similar distributions, corroborating the obscuration scenario.

While the obscuration scenario can be the solution for Radio Galaxies and Quasars, it may not be the general case for Seyfert 2 galaxies. Assuming that the [OII] emission in Seyfert 2's is similar to that of Seyfert 1's and not blocked by the torus, we can calculate, using the average values given in Table 3, that $\approx 40\%$ of the [NeIII] emission, $\approx 55\%$ of the [NeV] emission and $\approx 25\%$ of the [OIII] emission should be blocked by the torus in Seyfert 2's. This could happen for some of the Seyfert 2's in the sample, but notice that these are large values and go against the fact that Seyfert 2's have lower excitation lines (like [OII]) more luminous than Seyfert 1's of similar optical luminosity (Yee 1980; Shuder 1981). Also, Seyfert 2's usually have extended NLR's (Pogge 1989; Schmitt & Kinney 1996). Another fact that goes against the obscuration scenario being the general case is that, if part of the high excitation emission line region is hidden by the torus, we would expect to see considerable amounts of polarized [OIII] emission in Seyfert 2's. As shown by Goodrich (1992), with a small number of exceptions, Seyfert 2's do not have high degrees of polarized [OIII] emission.

2-) *We see a smaller number of ionization bounded clouds in Seyfert 1's, because they are seen from the back and are extincted.* Since the ionization bounded clouds are responsible for most of the [OII] emission and very little of the [NeIII], [NeV] and [OIII], this would imply a reduction of the ratios [OII]/[NeIII], [OII]/[NeV] and [OII]/[OIII] in Seyfert 1's, relative to Seyfert 2's.

From the analysis of the X-ray spectra of Seyfert 1's (Reynolds 1996; Weaver, Arnaud & Mushotzky 1995), it is known that they usually have small column densities of absorbing material ($N_{HI} < 10^{21} \text{ cm}^{-2}$). Assuming a standard dust-to-gas ratio ($A_V = 5 \times 10^{-22} N_{HI}$), it is possible to estimate a typical value of extinction from the above N_{HI} , which is $A_V < 0.5$ ($E(B-V) \approx 0.2$). In the case of $E(B-V) = 0.1$, the [OII] emission of the ionization bounded clouds would be reduced by $\approx 35\%$, which could explain the difference between Seyfert 1's and Seyfert 2's. However, this scenario only works when the ionization bounded clouds do not block the direct view of the matter bounded clouds, otherwise the high excitation lines would also be obscured.

3-) *There is a smaller number of ionization bounded clouds in Seyfert 1's, possibly due to the orientation of the circumnuclear torus relative to the galaxy plane.* In this scenario Seyfert 1's have their circumnuclear

torus axis preferentially aligned closer to the host galaxy plane axis, while in Seyfert 2's the torus can have any orientation. In this way, Seyfert 1's would have smaller NLR's, because their ionizing radiation would shine out of the galaxy disk and find only a small number of clouds to be ionized, thus resulting in a smaller number of ionization bounded clouds in these objects. On the other hand, since the Seyfert 2's torus axis can have any orientation relative to the host galaxy disk, there is a larger chance for the ionizing radiation to cross the galaxy disk in these objects, which would result in a larger quantity of gas clouds to be ionized. The clouds closer to the nucleus filter the ionizing radiation and the more distant clouds are ionized only by this fainter and filtered continuum. Due to the larger number of clouds along the disk, the nuclear radiation ionizes a larger number of clouds, and this effect is similar to seeing a larger number of ionization bounded clouds in Seyfert 2's.

Some of the results available in the literature, discussed in the introduction, corroborate this scenario. Seyfert 1's have higher [OIII]4363/5007 ratios than Seyfert 2's, which could be explained as higher [OIII] temperatures, or higher densities. If the higher [OIII]4363/5007 ratios of Seyfert 1's are in fact due to a higher [OIII] temperature, this is consistent with a smaller proportion of ionization bounded clouds in these objects, as shown by Binette et al. (1996) models. This interpretation can also explain the results obtained by Schmitt & Kinney (1996), that Seyfert 1's have much smaller NLR's than Seyfert 2's (when they are compared in a similar way, as if they were seen pole-on). Kraemer et al. (1998) confirmed this to the individual case of the Seyfert 1 galaxy NGC5548, showing that this galaxy has a compact NLR, with a size of the order of 70pc.

The above results imply that the NLR of Seyfert 1's have less gas than the NLR of Seyfert 2's, which can be explained if the Seyfert 1's torus axis is aligned closer to the host galaxy plane axis. This scenario is supported by the observation of a lack of Seyfert 1's in edge-on galaxies (Keel 1980; Maiolino & Rieke 1995; Simcoe et al. 1997) and by the relative orientation between linear radio structures and the host galaxy major axis in Seyfert 1's (Schmitt et al. 1997).

4-) *Seyfert 2's are more associated with circumnuclear star formation (high metallicity HII regions) than Seyfert 1's.* Since high metallicity HII regions are strong emitters of [OII] and weak emitters of [NeIII], if the nuclear emission of Seyfert 2's is more likely to be mixed with HII regions than Seyfert 1's, this would explain the fact that their NLR's show less excited gas. Some evidence for the existence of circumnuclear regions in Seyfert 2's is given by Heckman et al. (1995), Heckman et al. (1997), Thuan (1984). However, this evidence is restricted to a small number of galaxies and it would be necessary to study the stellar population of a complete sample of Seyfert 1's and Seyfert 2's, in order to see if there is any difference between these two classes of objects and if Seyfert 2's in fact have more circumnuclear star formation. One such attempt was done by Schmitt, Storchi-Bergmann & Cid Fernandes (1998), who synthesized the nuclear stellar population of 20 Seyfert 2's, showing that young stars usually contribute with less than 5% (less than 1% in more than 50% of the sample) to the light of these galaxies at $\lambda 5870\text{\AA}$.

5. Summary

This paper follows from a literature search of the fluxes of the emission lines [OII], [NeIII], [NeV], [OIII] and of the $60\mu\text{m}$ continuum for a sample of 52 Seyfert 1 and 68 Seyfert 2 galaxies. The analysis of possible selection effects shows that the two groups are not biased with respect to morphological type, have similar values of $60\mu\text{m}$ luminosity, and were observed with apertures of similar metric sizes.

The comparison between the distribution of the emission line ratios [OII]/[NeIII] and [OII]/[NeV]

in Seyfert 1's and Seyfert 2's, shows that the two groups are considerably different, with the Seyfert 2's spectra presenting more low excitation emission than the spectra of Seyfert 1's. The emission line ratios are compared with sequences of models in which only the ionization parameter varies, as well as with models which combine different proportions of matter and ionization bounded clouds. It is shown that the distribution of observed points can be better represented by the latter models, with Seyfert 1's having a smaller number of ionization bounded clouds than Seyfert 2's.

Four possible interpretations for this difference are proposed. The most likely explanation is that Seyfert 1's have smaller NLR's, thus have a smaller number of ionization bounded clouds. The NLR's of Seyfert 1's could be smaller than those of Seyfert 2's, due to an inclination effect. There is a growing amount of evidence, showing that the torus axis of Seyfert 1's is more likely to be aligned close to the galaxy plane axis, while in Seyfert 2's it can have any direction (Schmitt et al. 1997; Simcoe et al. 1997). In this way, the amount of gas ionized by the nuclear radiation would be smaller in Seyfert 1's than in Seyfert 2's, resulting in a larger number of ionization bounded clouds in these objects.

Two possibilities assume that part of the matter bounded clouds is hidden by the circumnuclear torus in Seyfert 2's, or that the ionization bounded clouds are seen from the back in Seyfert 1's, creating the impression that Seyfert 1's are more excited than Seyfert 2's. The evidence presented above go against these two scenarios as a general case. However, it is not possible to rule out individual cases where they could happen.

A fourth possibility assumes that Seyfert 2's have a larger number of circumnuclear star forming regions, relative to Seyfert 1's. There is some evidence of circumnuclear starformation in some Seyfert 2's. However, it still should be determined if this happens for all Seyfert 2's and if there is a difference between the stellar population of the two types of Seyferts.

It should be noticed that the results presented in this paper were obtained from a sample selected from the literature, rather than a sample selected from an isotropic property. Although it was shown that the two samples have similar intrinsic properties, there could still be some selection effects affecting the results. In order to avoid this, it would be important to test these results using homogeneous measurements of a sample selected by an isotropic property.

I would like to thank R. Antonucci, L. Binette, A. Kinney, T. Storchi-Bergmann, C. Winge and the anonymous referee for useful comments and suggestions. L. Binette is also thanked for making available the code MAPPINGS. This research has made use of the NASA/IPAC Extragalactic Database (NED) which is operated by the Jet Propulsion Lab, Caltech, under contract with NASA.

REFERENCES

- Alloin, D., Bica, E., Bonatto, C. J. & Prugniel, P. 1992, *A&A*, 266, 117
- Alloin, D., Pelat, D., Phillips, M. & Whittle, M. 1985, *ApJ*, 288, 205
- Anderson, K. S. 1970, *ApJ*, 162, 743
- Antonucci, R. R. J. & Miller, J. S. 1985, *ApJ*, 297, 621
- Antonucci, R. R. J. 1993, *ARA&A*, 31, 473
- Baldwin, J. A., Phillips, M. M. & Terlevich, R. 1981, *PASP*, 93, 5
- Binette, L., Wang, J. C. L., Zuo, L. & Magris, C. M. 1993a, *AJ*, 105, 797
- Binette, L., Wang, J. C. L., Villar-Martín, M., Martín, P. G. & Magris, C. M. 1993b, *ApJ*, 414, 535
- Binette, L., Wilson, A. S. & Storchi-Bergmann, T. 1996, *A&A*, 312, 365
- Boksenberg, A., Shortridge, K., Allen, D. A., Fosbury, R. A. E., Penston, M. V. & Savage, A. 1975, *MNRAS*, 173, 381
- Cohen, R. D. 1983, *ApJ*, 273, 489
- De Robertis, M. M. & Osterbrock, D. E. 1984, *ApJ*, 286, 171
- De Robertis, M. M. & Osterbrock, D. E. 1984, *ApJ*, 301, 727
- de Vaucouleurs, G., de Vaucouleurs, A., Corwin Jr., H. G., Buta, R. J., Paturel, G. & Fouque, P. 1991, *Third Reference Catalogue of Bright Galaxies*
- Diaz, A. I., Prieto, M. A., Wamsteker, W. 1988, *A&A*, 195, 53
- Durret, F. & Bergeron, J. 1986, *A&A*, 156, 51
- Durret, F. & Bergeron, J. 1988, *A&AS*, 75, 273
- Ferland, G. J. & Osterbrock, D. E. 1986, *ApJ*, 318, 145
- Filippenko, A. V. & Halpern, J. P. 1984, *ApJ*, 285, 458
- Gallimore, J. F., Baum, S. A., O’Dea, C. P., Brinks, E. & Pedlar, A. 1996, *ApJ*, 462, 740
- Gonzalez Delgado, R. M. & Perez, E. 1996, *MNRAS*, 280, 53
- Goodrich, R. W. 1992, *ApJ*, 399, 50
- Goodrich, R. W. & Osterbrock, D. E. 1983, *ApJ*, 269, 416
- Greenhill, L. J., Gwinn, C. R., Antonucci, R. & Barvainis, R. 1996, *ApJ*, 472, 21
- Heckman, T. M. & Balick, B. 1979, *A&A*, 79, 350
- Hes, R., Barthel, P. D. & Fosbury, R. A. E. 1993, *Nature*, 362, 326
- Jackson, N. & Browne, I. W. A. 1990, *Nature*, 343, 43
- Kay, L. 1994, *ApJ*, 430, 196
- Keel, W. C. 1980, *AJ*, 85, 198
- Koski, A. T. 1978, *ApJ*, 223, 56
- Kraemer, S. B., Crenshaw, D. M., Filippenko, A. V. & Peterson, B. M. 1998, *ApJ*, in press
- Kunth, D., Sargent, W. L. W. & Bothum, G. D. 1987, *AJ*, 93, 29
- Lipari, S., Tsvetanov, Z. & Macchetto, F. 1993, *ApJ*, 405, 186

- Maiolino, R. & Rieke, G. H. 1995, *ApJ*, 454, 95
- Miller, J. S. & Goodrich, R. W. 1990, *ApJ*, 355, 456
- Miyoshi, M., Moran, J., Herrnstein, J., Greenhill, L., Nakai, N., Diamond, P. & Inoue, M. 1995, *Nature*, 373, 127
- Moran, E. C., Halpern, J. P. Bothum, G. D. & Becker, R. H. 1992, *AJ*, 104, 990
- Morris, S. L. & Ward, M. J. 1988, *MNRAS*, 230, 639
- Mulchaey, J. S. 1994, PhD Thesis, University of Maryland
- Mulchaey, J. S., Mushotzky, R. F. & Weaver, K. A. 1992, *ApJ*, 390, L69
- Osterbrock, D. E. 1981, *ApJ*, 249, 462
- Osterbrock, D. E. 1985, *PASP*, 97, 25
- Osterbrock, D. E. & Dahari, O. 1983, *ApJ*, 273, 478
- Osterbrock, D. E. & Pogge, R. W. 1985, *ApJ*, 297, 166
- Pelat, D., Alloin, D. & Fosbury, R. A. E. 1981, *MNRAS*, 195, 787
- Phillips, M. M., Charles, P. A. & Baldwin, J. A. 1983, *ApJ*, 266, 485
- Pier, E. A. & Krolik, J. H. 1992, *ApJ*, 401,99
- Pogge, R. W. 1988a, *ApJ*, 328, 519
- Pogge, R. W. 1988b, *ApJ*, 332, 702
- Pogge, R. W. 1989, *ApJ*, 345, 730
- Reynolds, C. S. 1997, *MNRAS*, 286, 513
- Rodriguez-Ardila, A., Pastoriza, M. G., Bica, E. & Maza, J. 1996, *ApJ*, 463, 522
- Rola, C. S., Terlevich, E. & Terlevich, R. J. 1997, *MNRAS*, 289, 419
- Schmitt, H. R. & Storchi-Bergmann, T. 1995, *MNRAS*, 276, 592
- Schmitt, H. R., Storchi-Bergmann, T. & Baldwin, J. A. 1994, *ApJ*, 423, 237
- Schmitt, H. R., Storchi-Bergmann, T. & Cid Fernandes, R. 1998, in preparation
- Schmitt, H. R. & Kinney, A. L. 1996, *ApJ*, 463, 498
- Schmitt, H. R., Kinney, A. L., Storchi-Bergmann, T. & Antonucci, R. 1997, *ApJ*, 477, 623
- Simcoe, R., McLeod, K. K., Schachter, J. & Elvis, M. 1997, *ApJ*, 489, 615
- Shuder, J. M. 1980, *ApJ*, 240, 32
- Shuder, J. M. & Osterbrock, D. E. 1981, *ApJ*, 250, 55
- Shuder, J. M. & Osterbrock, D. E. 1981, *ApJ*, 250,55
- Storchi-Bergmann, T., Bica, E. & Pastoriza, M. G. 1990, *MNRAS*, 245, 749
- Storchi-Bergmann, T. & Pastoriza, M. G. 1989, *ApJ*, 347, 195
- Storchi-Bergmann, T., Wilson, A. S. & Baldwin, J. A. 1992, *ApJ*, 396, 45
- Terlevich, R., Melnick, J., Masegosa, J., Moles, M. & Copetti, M. V. F. 1991, *A&AS*, 91, 285
- Thuan, T. X. 1984, *Astrophys. J.*, 281, 126
- Tran, H. 1995, *ApJ*, 440, 565

- Tsvetanov, Z. & Walsh, J. R. 1992, *ApJ*, 386, 485
Ulvestad, J. S. & Wilson, A. S. 1983, *AJ*, 88, 253
Ulvestad, J. S. & Wilson, A. S. 1984a, *ApJ*, 278, 544
Ulvestad, J. S. & Wilson, A. S. 1984b, *ApJ*, 285, 439
Ulvestad, J. S. & Wilson, A. S. 1989, *ApJ*, 343, 659
Viegas, S. M. & Prieto, M. A. 1992, *MNRAS*, 258, 483
Ward, M., Penston, M. V., Blades, J. C. & Turtle, A. J. 1980, *MNRAS*, 193, 563
Weaver, K. A., Arnaud, K. A. & Mushotzky, R. F. 1995, *ApJ*, 447, 121
Wilson, A. S. & Penston, M. V. 1979, *ApJ*, 232, 389
Yee, H. K. C. 1980, *ApJ*, 241, 894

Fig. 1.— Comparison between the $60\mu\text{m}$ luminosity of Seyfert 1's (dotted line) and Seyfert 2's (solid line).

Fig. 2.— Comparison between the Morphological Types of the host galaxies of Seyfert 1's (dotted line) and Seyfert 2's (solid line).

Fig. 3.— Comparison between the $[\text{OII}]/[\text{NeIII}]$ distribution of Seyfert 1's (dotted line) and Seyfert 2's (solid line).

Fig. 4.— Comparison between the $[\text{OII}]/[\text{NeV}]$ distribution of Seyfert 1's (dotted line) and Seyfert 2's (solid line).

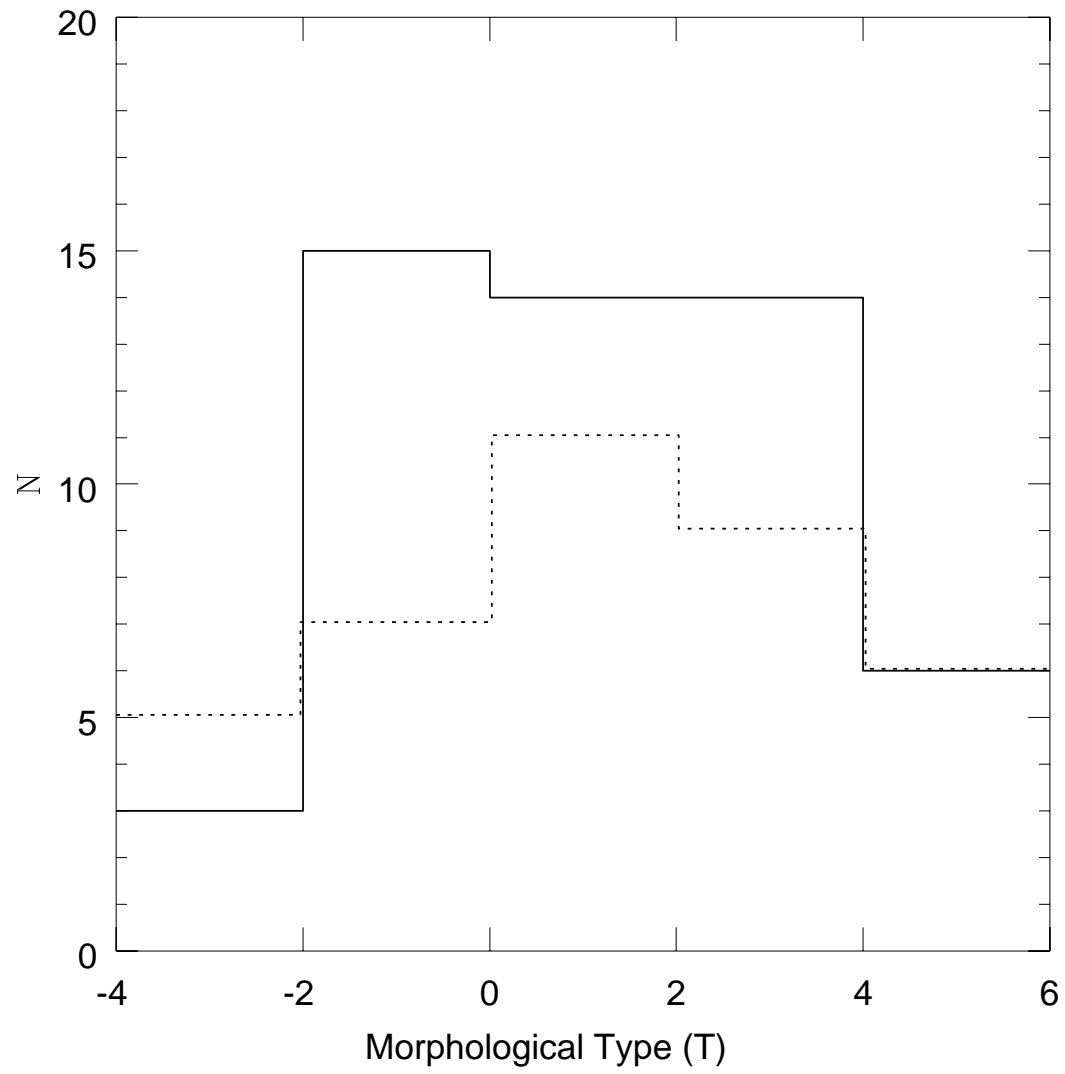
Fig. 5.— Comparison between the $[\text{NeIII}]/[\text{NeV}]$ distribution of Seyfert 1's (dotted line) and Seyfert 2's (solid line).

Fig. 6.— Comparison between the $[\text{OII}]/[\text{OIII}]$ distribution of Seyfert 1's (dotted line) and Seyfert 2's (solid line).

Fig. 7.— a-) Comparison between the emission line ratios $\text{Log } [\text{OII}]/[\text{NeV}] \times \text{Log } [\text{OII}]/[\text{NeIII}]$ and photoionization models. Open symbols are Seyfert 1's and filled symbols are Seyfert 2's. The solid lines represent the $A_{M/I}$ sequences of models with $n=50 \text{ cm}^{-3}$, $Z=1$, ionized by a power law continuum with slope $\alpha = -1.3$, or $\alpha = -1.5$, as indicated beside the line. The dashed lines represent the $A_{M/I}$ sequences of models ionized by power law spectra with $\alpha = -1.5$, but $n=500 \text{ cm}^{-3}$ and $Z=1$, or $n=50 \text{ cm}^{-3}$ and $Z=2$, as indicated beside the line by $n=500 \text{ cm}^{-3}$ and $Z=2$, respectively. $A_{M/I}$ was varied in the range $0.01 \leq A_{M/I} \leq 634$ in steps of 0.2 dex and decreases from left to right in the plot. The stars along the lines are separated by 0.2 dex and the large star corresponds to $A_{M/I} = 4$. Dotted line represents the sequence of ionization parameter models, calculated using a power law ionizing spectrum with $\alpha = -1.3$, $n=50 \text{ cm}^{-3}$ and $Z=1$. U was varied in the range $-4 \leq \text{Log } U \leq -0.8$ in steps of 0.2 dex. The stars along the line are separated by 0.2 dex, with the large star corresponding to $\text{Log } U = -2$.

Fig. 7.— b-) Same as Figure 7a, for the diagram $\text{Log } [\text{NeIII}]/[\text{NeV}] \times \text{Log } [\text{OII}]/[\text{NeIII}]$.

Fig. 7.— c-) Same as Figure 7a, for the diagram $\text{Log } [\text{OII}]/[\text{OIII}] \times \text{Log } [\text{OII}]/[\text{NeIII}]$. Due to the fact that the models with $\alpha = -1.3$ and $\alpha = -1.5$ are very similar, the plot only shows the models with $\alpha = -1.5$.



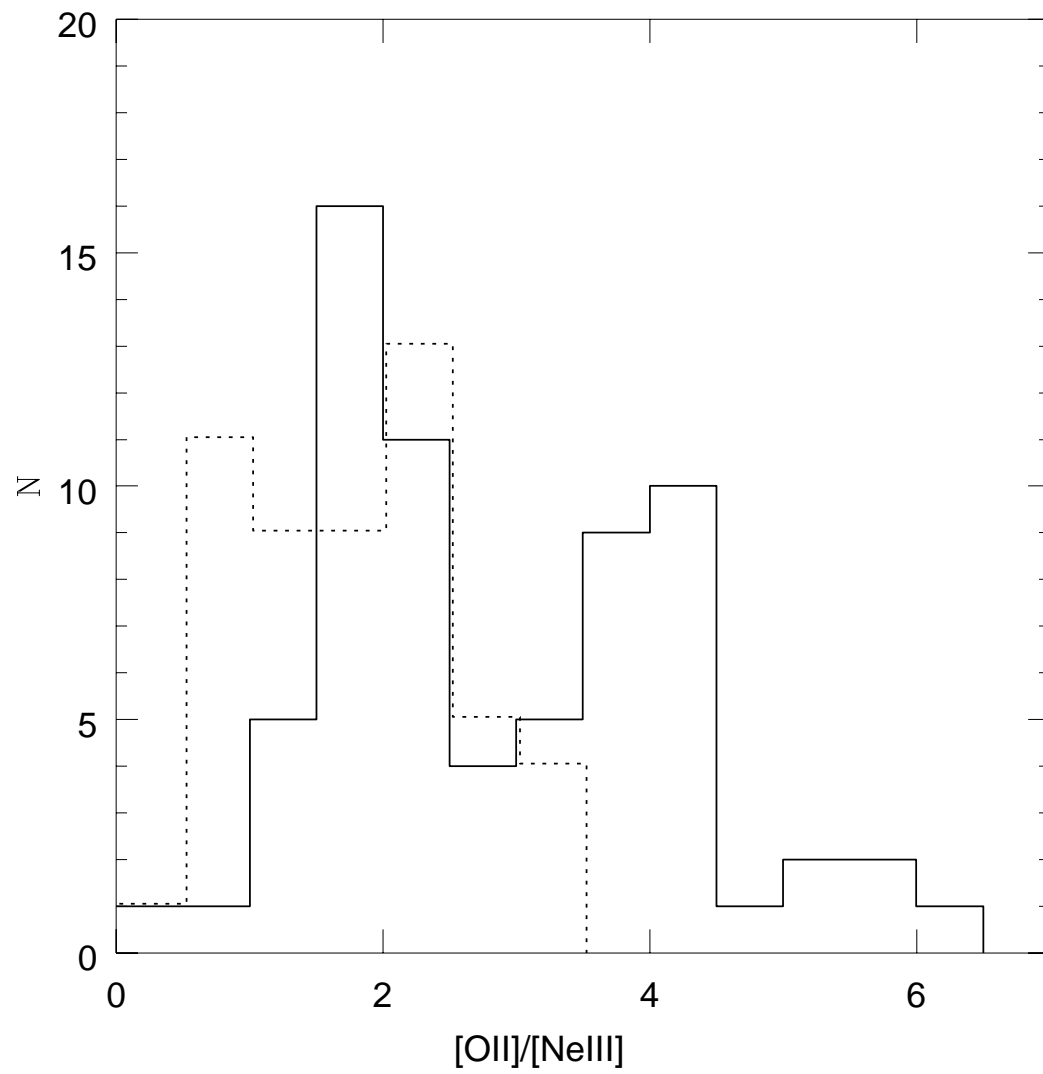


TABLE 1. Seyfert 1's

Name	B	V_0 km s ⁻¹	Morph.	[OII]/[NeIII]	[OII]/[NeV]	[NeIII]/[NeV]	[OII]/[OIII]	$F_{60\mu m}$ (Jy)	Ref.	Apert.
NGC 1019	14.95	7290	SBbc	2.955	—	—	0.210	0.355	12	M
NGC 1566	13.17	1290	SABbc	2.375	—	—	0.255	14.71	15	S
NGC 3227	13.52	990	SABa pc	1.603	5.05	3.150	0.177	7.825	22	S
NGC 3516	12.40	2700	SB0	0.667	0.857	1.286	0.126	1.758	16	L
NGC 3783	13.43	2880	SBa	0.414	0.861	2.080	0.081	3.257	14	M
NGC 4051	12.65	600	SABbc	1.571	1.100	0.700	0.292	7.131	16	L
NGC 4151	11.85	900	SABab	1.087	1.880	1.729	0.096	—	29	S
NGC 4253	13.60	3810	SB0/a	0.952	1.111	1.167	0.053	4.026	4	M
NGC 4593	13.15	2610	SBb	0.782	1.165	1.490	0.170	3.052	14	M
NGC 5033	10.75	892	SAC	2.727	—	—	0.600	13.8	26	S
NGC 5548	13.73	5100	SA0/a	2.579	0.547	0.212	0.098	1.073	22	S
NGC 6814	14.21	1590	SABbc	1.443	0.988	0.685	0.115	5.517	14	M
NGC 6860	13.50	4470	SBb	2.556	—	—	0.343	0.954	3	S
NGC 7450	14.33	3120	SBa	2.115	1.170	0.553	0.128	—	4	M
NGC 7469	13.15	4830	SABa	2.310	—	—	0.164	25.87	14	M
Mrk 6	14.19	5610	SAB0 ⁺	2.394	—	—	0.174	1.183	7	M
Mrk 42	15.28	7350	—	2.157	—	—	0.297	0.317	4	M
Mrk 79	14.02	6570	SBb	1.362	1.595	1.171	0.170	1.503	22	S
Mrk 279	14.46	9150	S0	3.224	—	—	0.427	1.255	22	S
Mrk 315	14.78	11820	S0/a pc	2.179	—	—	0.442	1.464	7	M
Mrk 359	14.22	5072	SB0	1.143	0.750	0.656	0.076	1.132	4	M
Mrk 372	14.81	9300	S0/a	2.046	—	—	0.253	0.303	7	M
Mrk 506	14.68	12900	SABa	3.136	—	—	0.153	—	22	S
Mrk 509	13.12	10650	E/S0	2.077	0.242	0.117	0.262	1.364	14	M
Mrk 595	14.69	8250	E/S0	1.769	—	—	0.230	—	17	M
Mrk 704	14.23	8730	Sa	0.509	0.348	0.684	0.082	0.364	22	S
Mrk 783	16.00	20000	—	3.167	—	—	0.296	0.31	4	M
Mrk 817	13.90	9600	S0/a pc	0.687	0.234	0.340	0.054	2.118	22	S
Mrk 841	14.85	10950	—	1.042	0.953	0.915	0.192	0.459	14	M
Mrk 871	14.80	10200	SB0	0.989	0.463	0.468	0.101	0.69	14	M
Mrk 896	14.61	7860	S?	1.543	0.679	0.440	0.152	0.513	14	M
Mrk 926	14.20	14400	Sa	2.133	5.818	2.727	0.312	—	23	S
Mrk 975	14.95	14730	S pec	0.541	0.338	0.625	0.063	0.8	22	S
Mrk 1018	14.30	12810	S0	1.636	—	—	0.180	—	25	S
Mrk 1239	14.39	5820	compact	1.050	—	—	0.150	1.335	4	M
Mrk 1320	15.00	30900	SBb	3.482	—	—	0.409	0.218	14	M
IC 4218	14.40	5820	Sb-c	1.536	—	—	0.232	—	14	M
IC 4329a	13.66	4800	S0 ⁺	1.2	—	—	0.028	2.03	28	S
MCG 8-11-11	14.00	6150	SBb-c	2	3.227	1.614	0.151	3.005	22	S
MCG-6-30-15	13.61	2340	E/S0	2.273	2.423	1.066	0.222	1.087	14	M
UM 146	14.50	5160	SAb	2.475	—	—	0.120	0.467	12	M
Fairall 51	14.10	4080	SBb	1.668	0.880	0.528	0.193	1.844	14	M
ESO 141-G55	13.60	11040	Sc	0.795	—	—	0.092	0.575	14	M
UGC 10683b	15.55	9200	—	1.421	0.231	0.163	0.145	0.479	14	M
TOL 0343-397	14.83	12900	E	1.692	—	—	0.321	0.24	13	L
TOL 1351-373	—	15500	—	1.476	1.594	1.080	0.107	0.45	14	M
TOL 1506.3-00	—	16200	—	2.039	2.676	1.312	0.204	—	14	M
TOL 20	—	7000	—	0.553	0.588	1.063	0.080	—	14	M
C 16.16	17.19	22864	—	2.3	3.286	1.429	0.217	—	5	S
E 1615+061	—	11370	—	2.789	6.092	2.185	0.301	—	14	M
H 1839-78	—	22200	—	0.778	0.348	0.447	0.162	—	14	M
IIIZw 77	—	10250	—	0.642	0.385	0.600	0.090	0.245	20	M

Morphological types were obtained from de Vaucouleurs et al. 1991 and Mulchaey 1994. Column 9 gives the references for the emission lines. 1-)Storchi-Bergmann, Bica, & Pastoriza 1990; 2-)Storchi-Bergmann & Pastoriza 1989; 3-)Lipari, Tsvetanov & Macchetto 1993; 4-)Osterbrock & Pogge 1985; 5-)Rodriguez-Ardila et al. 1996; 6-)Durret & Bergeron 1986; 7-)Koski 1978; 8-)Osterbrock 1985; 9-)Diaz, Prieto & Wamsteker 1988; 10-)Moran et al. 1992; 11-)Gonzalez Delgado & Perez 1996; 12-)Phillips, Charles & Baldwin 1983; 13-)Terlevich et al. 1991; 14-)Morris & Ward 1988; 15-)Alloin et al. 1985; 16-)Anderson 1970; 17-)Ulvestad & Wilson 1983; 18-)Shuder & Osterbrock 1981; 19-)Osterbrock & Dahari 1983; 20-)Ferland & Osterbrock 1986; 21-)Goodrich & Osterbrock 1983; 22-)Cohen 1983; 23-)Durret & Bergeron 1988; 24-)Kunth, Sargent & Bothum 1987; 25-)Osterbrock 1981; 26-)Shuder 1980; 27-)Ward et al. 1980; 28-)Wilson & Penston 1979; 29-)Boksenberg et al. 1975; 30-)Alloin et al. (1992).

TABLE 2. Seyfert 2's

Name	B	V_0 km s ⁻¹	Morph.	[OII]/[NeIII]	[OII]/[NeV]	[NeIII]/[NeV]	[OII]/[OIII]	$F_{60\mu m}$ (Jy)	Ref.	Apert.
NGC 424	14.12	3300	SB0/a	1.310	—	—	0.130	1.796	22	S
NGC 1068	10.83	1020	Sb	0.809	1.056	1.306	0.058	181.95	7	M
NGC 1229	14.00	10590	SBb pec	4.179	3.836	0.918	0.263	1.548	12	M
NGC 1358	13.05	3870	SAB0/a	4.253	—	—	0.387	0.378	2	L
NGC 1386	12.84	810	Sa/S0	2.810	—	—	0.177	5.396	2	L
NGC 1667	12.77	4472	Sc	5.182	—	—	0.371	5.952	12	M
NGC 2110	13.51	2130	SA0	4.300	—	—	0.430	4.129	26	S
NGC 2992	13.78	2250	Sa pec	4.623	—	—	0.319	6.760	1	L
NGC 3081	13.55	2160	SAB0/a	1.949	1.086	0.557	0.164	—	6	S
NGC 3281	14.02	3540	SAa	3.022	3.886	1.286	0.245	6.861	23	S
NGC 3393	12.40	3690	Sa	4.179	—	—	0.148	2.251	9	M
NGC 3786	13.74	2760	SABa pc	3.553	—	—	0.270	—	21	S
NGC 3982	11.70	10800	SABb	2.056	—	—	0.153	6.567	12	M
NGC 4074	14.44	6600	S0 pec	1.818	1.471	0.809	0.100	—	18	S
NGC 4388	11.76	2545	SAb	5.586	—	—	0.324	10.240	1	L
NGC 4507	13.54	3480	SBab	3.921	4.798	1.224	0.265	4.310	6	S
NGC 4941	12.23	870	SABab	4.079	—	—	0.257	1.378	2	L
NGC 4939	13.80	2910	SAbc	1.484	—	—	0.095	2.015	1	L
NGC 5135	13.35	3990	SBab	2.524	—	—	0.220	16.910	12	M
NGC 5256	13.42	8280	S0 pec	5.446	—	—	0.635	7.342	19	S
NGC 5347	12.70	2370	SBab	1.848	1.525	0.825	0.508	1.424	11	S
NGC 5506	14.38	1830	Sa pec	3.586	9.369	2.613	0.267	8.409	14	M
NGC 5643	13.60	990	SABc	1.844	1.895	1.028	0.152	19.490	14	M
NGC 5728	13.40	2790	SABa	2.453	5.257	2.143	0.156	8.163	12	M
NGC 6300	13.08	900	SBb	2.491	—	—	0.279	14.650	2	L
NGC 6890	14.02	2430	SAb	1.081	—	—	0.107	3.855	1	L
NGC 7130	13.87	4830	Sa pec	2.442	—	—	0.188	16.480	1	L
NGC 7314	13.11	1500	SABbc	2.401	2.290	0.954	0.139	3.736	14	M
NGC 7582	13.57	1560	SBab	1.745	6.584	3.772	0.258	49.100	27	M
NGC 7743	13.28	2040	SB0/a	1.871	—	—	0.595	0.791	2	L
Mrk 1	14.96	4800	SB0/a	1.491	3.286	2.204	0.137	2.531	7	M
Mrk 3	13.34	4110	E2 pec	2.351	—	—	0.164	3.770	7	M
Mrk 34	14.76	15450	S	3.000	—	—	0.220	0.809	7	M
Mrk 78	15.00	11145	E/S0	2.383	—	—	0.196	1.110	7	M
Mrk 176	14.61	8070	S0/a pc	1.111	—	—	0.108	0.694	7	M
Mrk 198	14.73	7170	SAB0 pc	4.370	—	—	0.351	0.624	7	M
Mrk 268	14.66	12300	Sa	4.410	—	—	0.535	1.381	7	M
Mrk 270	14.05	3090	SAB0	3.943	—	—	0.541	—	7	M
Mrk 348	13.90	4410	SA0/a	2.480	—	—	0.247	1.290	7	M
Mrk 423	14.29	9720	S0?	3.591	—	—	0.790	1.423	25	S
Mrk 463e	14.22	15150	S pec	3.231	—	—	0.210	2.184	18	S
Mrk 516	16.50	8519	—	3.765	—	—	0.640	1.325	25	S
Mrk 573	14.07	5130	SAB0	2.089	—	—	0.167	1.088	7	M
Mrk 609	14.12	10260	E/S0	1.545	3.333	2.157	0.170	2.550	25	S
Mrk 612	15.50	6206	SB0/a?	1.864	—	—	0.110	1.159	18	S
Mrk 622	14.40	6840	S0 pec	7.656	—	—	0.490	1.281	18	S
Mrk 1066	14.01	3540	SB0	4.211	—	—	0.320	10.98	21	S
Mrk 1193	16.50	9600	—	3.355	—	—	0.190	0.641	13	L
Mrk 1388	15.70	6390	—	0.473	—	—	0.048	0.174	8	S
IC 1515	14.80	6870	SBb	1.524	0.976	0.641	0.170	0.566	12	M
IC 5063	13.60	3300	SA0a pc	3.656	—	—	0.223	5.337	1	L
MCG-5-23-16	13.69	2280	S0	1.533	1.769	1.154	0.110	—	23	S
UM 16	17.00	17400	—	1.605	2.653	1.653	0.130	—	18	S
UM 82	17.88	15300	—	1.802	—	—	0.095	—	13	L
UM 85	17.29	12300	—	3.293	—	—	0.174	—	13	L
UM 103	17.00	13500	—	3.113	—	—	0.280	—	13	L
UM 293	16.40	16800	—	2.804	—	—	0.239	—	13	L
Fairall 4	15.10	15900	Sb	1.579	—	—	0.101	—	13	L
ESO 138-G1	14.31	2730	E/S0	2.219	1.426	0.643	0.193	—	30	M
ESO 103-G35	14.53	4050	S0?	5.651	—	—	0.365	2.314	14	M
TOL0514-415	—	14700	—	4.154	—	—	0.300	—	13	L
TOL0544-395	14.90	7500	S0	3.584	—	—	0.239	0.917	13	L
TOL0611-375	—	11400	—	4.115	—	—	0.213	—	13	L
WAS 49a	—	18900	—	1.923	5.263	2.737	0.101	0.438	10	S
POX 52	17.20	6420	—	3.509	8.000	2.280	0.288	—	24	M
IZw 92	15.20	11340	—	2.062	3.448	1.672	0.200	1.313	18	S
IIIZw 55	15.40	7507	—	1.928	—	—	0.172	0.867	7	M
VZw 317	15.77	10200	—	1.571	—	—	0.660	—	25	S

Morphological types were obtained from de Vaucouleurs et al. 1991 and Mulchaey 1994. The references correspond to the same number as in Table 1.

TABLE 3. Comparison between Seyfert 1's and Seyfert 2's

Ratio	Sy1	Mean	STD	Sy 2	Mean	STD	P(%)
$60\mu\text{m}$	40	43.61	0.48	52	43.71	0.60	43.74
Morph Types	37	—	—	52	—	—	99.86
[OII]/[NeIII]	52	1.73	0.81	68	2.91	1.37	0.02
[OII]/[OIII]	52	0.19	0.11	68	0.26	0.16	22.59
[OII]/[NeV]	31	1.54	1.6	21	3.49	2.35	0.16
[NeIII]/[NeV]	31	1.05	0.74	21	1.55	0.85	10.87

Column 1 gives the quantity that is being analysed, column 2(5), 3(6) and 4(7) give the number of Seyfert 1's (Seyfert 2's) with the measurement available, their average value and standard deviation, respectively. Column 8 gives the KS test significance for rejection of the hypothesis that the two distributions are drawn from the same population.

